

Contributions of Resonant Excitation Double Autoionization to the Electron-Impact Ionization of Fe^{15+}

M. H. Chen and K. J. Reed

High Temperature Physics Division, Lawrence Livermore National Laboratory, Livermore, California 94550

D. L. Moores^(a)

Department of Physics, Auburn University, Auburn, Alabama 36899

(Received 2 January 1990)

Electron-impact ionization cross sections for Fe^{15+} have been calculated using relativistic distorted-wave methods. We have performed the most comprehensive calculation to date by including more than 10000 autoionizing levels for resonant-excitation double-autoionization (REDA) processes. The total cross sections exhibit many strong narrow resonances. The REDA process contributes about 30% to the average total cross sections. General good agreement between theory and experiment is attained, but new experimental investigations are needed to search for the predicted resonances.

PACS numbers: 34.80.Kw, 32.80.Dz

Electron-impact ionization of multiply charged ions is an important ionization process in hot dense plasmas. It affects ionization balance, electron density and temperature, and the plasma kinetics as well. In the last decade, much effort has been spent in both theory and experiment to obtain ionization cross sections for highly charged ions which are relevant to astrophysics and fusion research. These intense studies have revealed that indirect processes frequently make far greater contributions to the ionization cross sections than does the direct ionization process.¹⁻³ The most important indirect process contributing to the single ionization by electron impact is excitation of an inner-shell electron followed by Auger decay. Higher-order processes such as resonant excitation followed by emission of two electrons in two steps [resonant excitation double autoionization (REDA)]^{4,5} or in a single step (READI)⁶ have also been computed and experimentally observed for a few cases.^{7,8}

The sodium isoelectronic sequence has become a testing ground for the study of indirect ionization processes because of its simple atomic structure. In theoretical investigations of indirect ionization processes, Moores and Nussbaumer⁹ used a Coulomb-Born approximation while Griffin, Bottcher, and Pindzola,¹⁰ Cowan and Mann,¹¹ and LaGattuta and Hahn⁴ employed distorted-wave approximations. Close-coupling calculations have also been carried out by Henry and Msezane,⁵ and Tayal and Henry.¹² On the experimental front, Crandall *et al.*¹³ measured absolute total ionization cross sections for few time ionized Na-like ions, and Gregory *et al.*¹⁴ obtained absolute total ionization cross sections for Fe^{15+} . These investigations concentrated on ions with atomic number $Z \leq 28$. Recently, ions as heavy as Au^{68+} have also been treated theoretically.¹⁵ All of these studies indicate that excitation-autoionization cross sections are about 4 times the direct ionization cross sections.

Higher-order processes such as REDA and READI were not included in most of these earlier theoretical investigations. For Fe^{15+} , LaGattuta and Hahn,⁴ using a configuration-average model, predicted that the REDA process enhances the direct ionization cross section by more than a factor of 5 for impact electron energies in the range $750 \leq E \leq 780$ eV. A subsequent experimental measurement¹⁴ failed to confirm the large predicted enhancement.⁴ Instead, large fluctuations in cross sections as a function of electron energy were observed. Later, Tayal and Henry¹² performed a close-coupling calculation and concluded that REDA contributes very little to the ionization cross sections. However, in their treatment of REDA processes Tayal and Henry¹² only included contributions from the $2p^5 3s 3nl'$ Rydberg series. Furthermore, radiative decays were neglected in the first step of this two-step process, and not all possible Auger channels were included in their calculations of branching ratios for the first step.

In order to shed some light on the importance of the REDA ionization process for Fe^{15+} , we carried out the first comprehensive calculations of the REDA cross sections using a detailed multiconfiguration Dirac-Fock model (MCDF).^{16,17} We include more than 10000 intermediate autoionizing levels in the calculations. Direct ionization and excitation-autoionization cross sections were also computed using relativistic distorted-wave methods.^{18,19}

The need for performing extension level-to-level calculations for indirect ionization processes has been indicated in results of earlier calculations. For example, in their calculation of excitation-autoionization cross sections for Fe^{15+} , Griffin, Bottcher, and Pindzola¹⁰ found that Auger branching ratios are very sensitive to configuration-interaction and to intermediate coupling effects. In addition, the configuration-average approximation has been shown to underestimate the average L -

shell fluorescence yields for Fe^{15+} by a factor of 4.²⁰

In the distorted-wave calculations of electron-impact ionization for Fe^{15+} , we consider an excitation-autoionization process with excitation of a $2p$ electron into the $n=3$ or $n=4$ shell or excitation of a $2s$ electron into the $n=3$ shell;

$$e + 1s^2 2s^2 2p^6 3s \rightarrow 1s^2 2s^2 2p^5 3s n l (n=3,4) + e \rightarrow 1s^2 2s^2 2p^6 + e + e \quad (1)$$

and

$$e + 1s^2 2s^2 2p^6 3s \rightarrow 1s^2 2s 2p^6 3s 3l + e \rightarrow 1s^2 2s^2 2p^6 + e + e. \quad (2)$$

We also include contributions from the $1s^2 2s^2 2p^5 3p^2$ states which can be excited by configuration interaction.

The REDA ionizing process can be represented schematically by

$$e + 1s^2 2l^8 3s \rightarrow 1s^2 2l^7 3s n l n' l' \rightarrow 1s^2 2l^7 3s n'' l'' + e \rightarrow 1s^2 2s^2 2p^6 + e + e. \quad (3)$$

We carried out explicit calculations for resonant states from $2s^2 2p^5 3s 4l n l' (n=4-7)$, $2s^2 2p^5 3s 3l n l' (n=7-12)$, $2s 2p^6 3s 3l n l' (n=4-10)$, $2p 2p^6 3s 4l l'$, and $2s^2 2p^5 3s 5l l'$ configurations. For the first three cases, extrapolation to $n=30$ was accomplished by using a n^{-3} scaling law for the Auger transitions. The READI process is not treated in our calculations.

Assuming that the direct and indirect ionization processes are independent, the total cross section σ_i is given by

$$\sigma_i = \sigma_d + \sum_i \sigma_i^{\text{ex}} B_i^a + \sum_k \bar{\sigma}_k^{\text{cap}} B_k^{da}, \quad (4)$$

where σ_d is the direct ionization cross section; σ_i^{ex} and $\bar{\sigma}_k^{\text{cap}}$ are excitation and energy-averaged capture cross sections, respectively; B_i^a and B_k^{da} are the branching ratios for the single and double Auger emission, respectively. The single and sequential double Auger branching ratios can be written as

$$B_i^a = \frac{\sum_j A_{ij}^a}{\sum_m A_{im}^a + \sum_k A_{ik}^a}, \quad (5)$$

and

$$B_k^{da} = \frac{\sum_{k'} A_{k'k}^a \sum_f A_{k'f}^a}{(\sum_m A_{km}^a + \sum_n A_{kn}^a)(\sum_m A_{k'm}^a + \sum_n A_{k'n}^a)}, \quad (6)$$

where A_{ij}^a and A_{ik}^a are the Auger transition from state i to j and radiative decay rate from state i to k , respectively.

The energy-averaged dielectronic capture cross section in cm^2 is obtained from the inverse Auger process by de-

tailed balance:⁴

$$\bar{\sigma}_k^{\text{cap}} = \frac{4.95 \times 10^{-30}}{\Delta E E_k} \frac{g_k}{2g_i} A_{ki}^a. \quad (7)$$

Here, ΔE and E_k are, respectively, the energy bin and Auger energy in eV; g_k and g_i are the statistical weights for the intermediate state k and the initial state i , respectively.

The direct ionization cross section is evaluated using a full partial-wave expansion method¹⁸ in which the bound, incident, scattered, and ejected electron wave functions are calculated in Dirac-Fock potentials.¹⁷ Exchange is included by using completely antisymmetric final-state wave functions in the ionization amplitude.

The inner-shell excitation cross sections were computed using a relativistic distorted-wave approximation.¹⁹ Relativistic configuration-interaction (CI) wave functions for the Na-like target were generated using a Dirac-Fock atomic-structure code developed by Hagelstein and Jung.¹⁹ We included the $2s^2 2p^6 3l$, $2s^2 2p^5 3l 3l'$, and $2s 2p^6 3l 3l'$ states in the CI calculation of the target wave functions.

The detailed Auger and radiative rates required in calculations of capture cross sections and branching ratios [Eqs. (5)-(7)] were computed using the MCDF model.¹⁶ The energy levels and wave functions for the excited states were calculated explicitly in intermediate coupling, including configuration interaction within the same complex using the MCDF model in the average-level scheme.¹⁷

We have calculated the electron-impact ionization cross sections for Fe^{15+} with incident electron energy $600 \leq E \leq 1000$ eV using the multiconfiguration distorted-wave method. The contributions from the indirect processes were obtained by multiplying the excitation or capture cross sections by the appropriate branching ratios. The total cross sections were computed according to Eq. (4). Our results are displayed in Fig. 1. The direct ionization cross sections (dashed curve) exhibit smooth dependence on impact electron energy. In the excitation-autoionization calculation, we included eighty intermediate states in $n=2$ to $n=3$ excitation and forty states in $n=2$ to $n=4$ excitation. For $n=2$ to $n=3$ excitation, eight intermediate states together contribute 70% of the total excitation-autoionization cross sections at $E=977$ eV. For Fe^{15+} , $2p-3d$ excitation contributes as much as the $2p-3p$ excitation in contrast to the case of Au^{68+} which is dominated by the $2p-3p$ excitation¹⁵ due to the strong $2p-3d$ radiative electric-dipole transition. Above $E=950$ eV, $n=2$ to $n=4$ excitation contributes about 10% of the total ionization cross section. For electron energy $E \geq 820$ eV, excitation-autoionization cross section is about a factor of 4 larger than the direct ionization cross section (see Fig. 1). Including detailed radiative decay rates in the calculations of branching ratios reduces the excitation-autoionization cross sections by

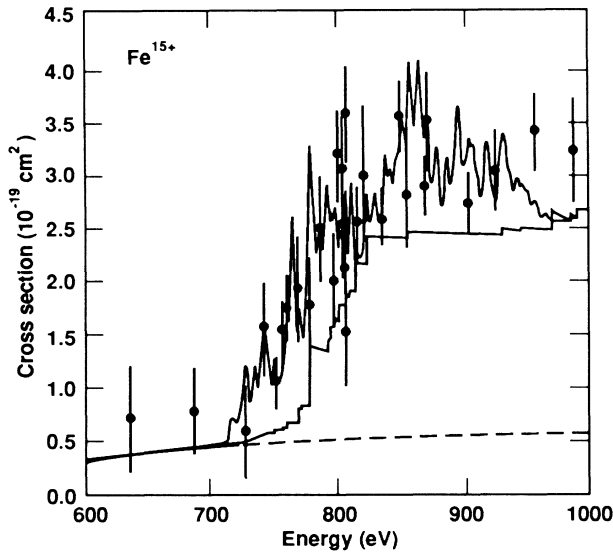


FIG. 1. Electron-impact ionization cross sections from the present MCDF calculations are compared with experiment. The dashed curve shows the direct ionization cross sections. The lower solid curve represents total cross sections with excitation autoionization. The upper solid curve indicates the total cross sections including REDA contributions as well. The dots with error bars are experiment (Ref. 14).

40%.

Our direct ionization cross sections are about 10% smaller than the cross sections computed using Lotz's formula,²¹ but are within 5% of the results of other distorted-wave calculations.^{10,22} The excitation-autoionization cross sections from the present work are within 10% of the existing theoretical results^{10,23} except near the threshold region ($E < 800$ eV). In this energy region, the excitation-autoionization cross sections from the configuration-average calculations²³ are larger than our detailed level calculations by as much as a factor of 3 due to the fact that not all states from the same configuration are energetically accessible.

For the REDA process, we have performed the most comprehensive calculations to date. We included more than 10000 autoionizing levels by using the detailed MCDF model. In the calculations of the two-step double Auger branching ratios B_k^{da} [Eq. (6)], all possible Auger channels and radiative decays leading to bound states were taken into account. The REDA cross section is diminished by about 50% due to the inclusion of radiative transitions. To facilitate the comparison with experiment,¹⁴ each REDA resonance is convoluted with a Gaussian of 2 eV in width. The total ionization cross section obtained by adding the excitation-autoionization and REDA cross sections to the direct ionization cross section shows complex resonance structure due to the REDA process (upper solid curve in Fig. 1). The peaks below 750 eV arise from intermediate states $2p^5 3s 3nl'$ ($n=7-9$). The strong peaks between 760 and 800 eV

and those between 800 and 850 eV are mainly due to the $2p^5 3s 4l'$ and $2s 2p^6 3nl'$ ($n=5-10$) states, respectively. For electron energy $E \geq 850$ eV, the $2p^5 3s 4nl'$ ($n \geq 5$) states are responsible for the resonance structure.

For the purpose of comparison, the experimental cross sections are also shown in Fig. 1. The overall agreement between our theoretical predictions and experiment is rather good. Some narrow strong peaks at $E=760, 780, 858,$ and 865 eV, in particular, might have been missed by the experimental observation.¹⁴ For $E > 950$ eV, the two experimental points lie above the theoretical results by 15%. These discrepancies may be partly due to the neglect of the contributions from $n=2$ to $n=5$ excitation autoionization and from $2s 2p^6 3s 4nl'$ ($n \geq 5$) intermediate states in REDA calculations.

In Fig. 2, the theoretical cross sections from our present work are compared with the predictions from configuration-average approximation⁴ and the close-coupling method.¹² The total ionization cross sections from our present MCDF calculations show many resonance peaks due to the inclusion of the REDA cross sections obtained by the detailed calculations. For electron energy $E \geq 820$ eV, the average cross sections from these three theories agree within 20%. For $750 \leq E \leq 800$ eV, the cross sections from the configuration-average approximation⁴ with a 20-eV bin width are a factor of 2 to 3 larger than our MCDF predictions. If a 2-eV bin width had been used in Ref. 4 as was done in this work, the resonance peaks from the configuration-average calculations would be more than an order of

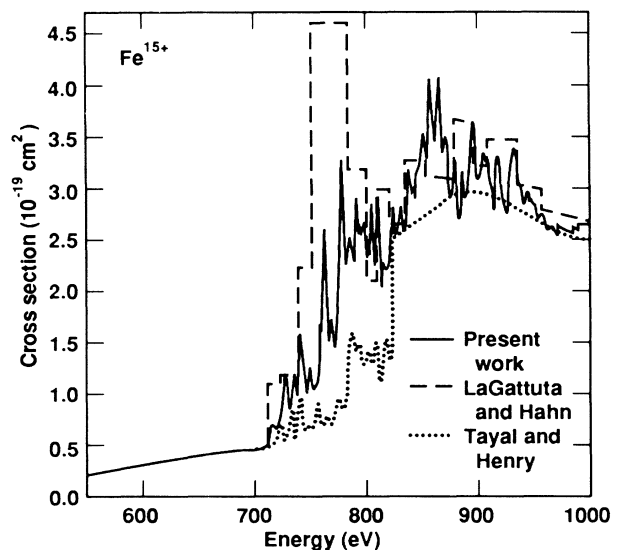


FIG. 2. Theoretical electron-impact ionization cross sections as functions of electron energy. The solid curve displays the present MCDF results. The dotted curve represents the values from the close-coupling calculations (Ref. 12) and the dashed curve shows the predictions from the configuration-average approximation (Ref. 4).

magnitude larger than our results from detailed calculations. This clearly demonstrates the importance of performing detailed level-to-level calculations in the treatment of the REDA processes. The cross sections from the close-coupling calculations¹² for $750 \leq E \leq 800$ eV are a factor of 2 smaller than the values from our present work. These discrepancies are mostly due to the fact that Tayal and Henry¹² included only the $2p^5 3s 3nl'$ Rydberg series in their REDA calculations. We have shown that the most important contributions to the REDA cross sections in these energy ranges arise from the $2p^5 3s 4l4l'$ and $2s 2p^6 3s 3nl'$ intermediate states which were neglected in the close-coupling calculations.¹²

In this work, we have calculated direct, excitation-autoionization and REDA cross sections for Fe^{15+} using a detailed MCDF model. Our REDA cross sections are smaller than the results calculated by LaGattuta and Hahn,⁴ but larger than the values obtained by Tayal and Henry.¹² We conclude that the REDA process contributes about 30% to the average total ionization cross sections for Fe^{15+} with impact electron energy $720 \leq E \leq 940$ eV. The REDA processes are manifested by a number of strong narrow resonances. The large fluctuations shown in experimental measurements¹⁴ may be associated with the REDA resonances. We call for new experiments to search for these strong narrow resonances.

This work was performed under the auspices of the U.S. Department of Energy by the Lawrence Livermore National Laboratory under Contract No. W-7405-ENG-48.

^(a)Permanent address: Department of Physics and Astrono-

my, University College London, Gower Street, London WC1E 6BT, England.

¹R. A. Falk *et al.*, Phys. Rev. Lett. **47**, 494 (1981).

²R. K. Feeney, J. W. Hooper, and M. T. Elford, Phys. Rev. A **6**, 1469 (1972).

³D. C. Griffin *et al.*, Phys. Rev. A **29**, 1729 (1984).

⁴K. T. LaGattuta and Y. Hahn, Phys. Rev. A **24**, 2273 (1981).

⁵R. J. W. Henry and A. Z. Msezane, Phys. Rev. A **26**, 2545 (1982).

⁶M. S. Pindzola and D. C. Griffin, Phys. Rev. A **36**, 2628 (1987).

⁷A. Müller, K. Tinschert, G. Hofmann, E. Salzborn, and G. H. Dunn, Phys. Rev. Lett. **61**, 70 (1988).

⁸A. Müller, G. Hofmann, K. Tinschert, and E. Salzborn, Phys. Rev. Lett. **61**, 1352 (1988).

⁹D. L. Moores and H. Nussbaumer, J. Phys. B **3**, 6 (1970).

¹⁰D. C. Griffin, C. Bottcher, and M. S. Pindzola, Phys. Rev. A **25**, 154 (1982); **36**, 3642 (1987).

¹¹R. D. Cowan and J. B. Mann, Astrophys. J. **232**, 940 (1979).

¹²S. S. Tayal and R. J. W. Henry, Phys. Rev. A **39**, 3890 (1989).

¹³D. H. Crandall *et al.*, Phys. Rev. A **25**, 143 (1982).

¹⁴D. C. Gregory, L. J. Wang, F. W. Meyer, and K. Rinn, Phys. Rev. A **35**, 3256 (1987).

¹⁵K. J. Reed, M. H. Chen, and D. L. Moores, Phys. Rev. A **41**, 550 (1990).

¹⁶M. H. Chen, Phys. Rev. A **31**, 1449 (1985).

¹⁷I. P. Grant *et al.*, Comput. Phys. Commun. **21**, 207 (1980).

¹⁸D. L. Moores (unpublished).

¹⁹P. L. Hagelstein and R. K. Jung, At. Data Nucl. Data Tables **37**, 17 (1987).

²⁰M. H. Chen, Phys. Rev. A **40**, 2758 (1989).

²¹W. Lotz, Z. Phys. **216**, 341 (1968).

²²S. M. Younger, Phys. Rev. A **24**, 1272 (1981).

²³A. L. Mertz *et al.*, Los Alamos Scientific Laboratory Report No. LA-8267-MS, 1980 (unpublished), as reported in Ref. 4.